

# Optimization of Quantum Trajectories Driven by Strong-Field Waveforms

S. Haessler<sup>1,\*</sup>, T. Balciūnas<sup>1</sup>, G. Fan<sup>1</sup>, T. Witting<sup>2</sup>, R. Squibb<sup>2</sup>, L. Chipperfield<sup>3</sup>, A. Zair<sup>2</sup>, G. Andriukaitis<sup>1</sup>,  
A. Pugžlys<sup>1</sup>, J. W. G. Tisch<sup>2</sup>, J. P. Marangos<sup>2</sup>, A. Baltuška<sup>1</sup>

<sup>1</sup> Photonics Institute, Vienna University of Technology, Gusshausstrasse 27/387, 1040 Vienna, Austria

<sup>2</sup> Blackett Laboratory, Imperial College, London SW7 2AZ, United Kingdom

<sup>3</sup> Max Born Institute, Max-Born-Straße 2 A, 12489 Berlin, Germany

**Abstract:** We combine phase-locked femtosecond pulses with 1.5 $\mu\text{m}$ , 1.0 $\mu\text{m}$  and 0.5 $\mu\text{m}$  wavelength to shape optical cycles and experimentally realize the concept of the “perfect wave for high harmonic generation”. This has far-reaching implications for attosecond spectroscopy.

**OCIS codes:** (270.6620) Strong-field processes, (020.2649) Strong field laser physics, (140.7090) Ultrafast Lasers

Recently, with the generation and amplification of phase-locked more-than-octave spanning spectra, the capability for sub-cycle waveform shaping has been demonstrated [1] and applied for the sub-femtosecond confinement of field ionization to a single field crest [2]. Here we apply shaped optical cycles, synthesized from a 1.6-octave-spanning spectrum, to a more complex optimization task, the efficient acceleration and return of the ionized electron in HHG. As illustrated in Fig. 1, we address a fundamental bottleneck in HHG driven by sinusoidal driver waves: drive wavelength,  $\lambda$ , and intensity,  $I$ , combine to the highest achievable electron energy at recollision,  $3.2U_p$ , where  $U_p \propto I\lambda^2$ . The intensity is limited to a small range due to the combined effect of the exponentially growing ionization rate and saturation (unity ionization probability), while an increasing wavelength leads to a drop  $\propto \lambda^{-6}$  of the conversion efficiency [3]. This is mainly due to the increased trajectory excursion duration,  $\propto \lambda$ , which causes additional quantum wave packet spreading and reduces the recollision amplitude. Here, applying shaped optical cycles we tailor the single-atom quantum dipole to demonstrate the efficacy of the “perfect wave” concept [4] and so take an important step towards the removal of the above-mentioned bottleneck.

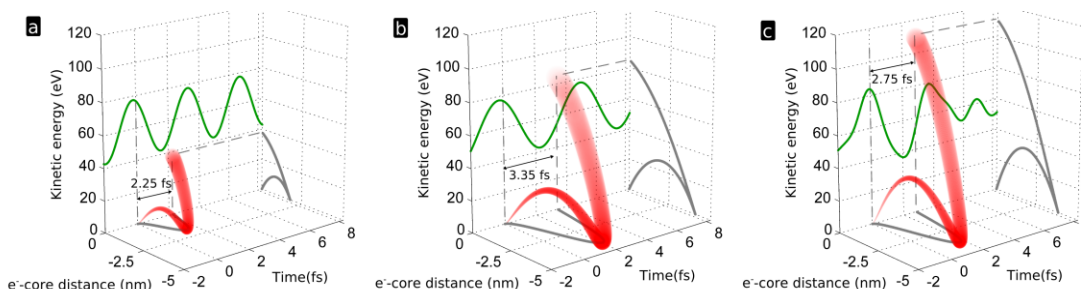


**Fig. 1:** Simulated optimization of HHG via the driving waveform. The driving electric field is shown by the green line. Both single-color drivers [1.03  $\mu\text{m}$  (a) and 1.545  $\mu\text{m}$  (b)] have an intensity of  $1.2 \times 10^{14} \text{ W cm}^{-2}$ . The 3-color waveform [(c), combination of 1.03  $\mu\text{m}$ , 0.515  $\mu\text{m}$  and 1.545  $\mu\text{m}$  with relative intensities as in our experiments (Fig. 3) and optimal phase delays] has the same fluence within its 10.3-fs period as the single-color waves. The cutoff electron trajectory, leading to the highest recollision energy and thus highest emitted HHG photon energy is shown by points with radii that linearly increase with excursion time, symbolizing wavepacket spreading. The optimized 3-color-driver leads to enhanced acceleration of the continuum electron during a shorter excursion time, thus mitigating wavepacket spreading.

Furthermore, the field strength launching the trajectories by tunnelling ionization is enhanced.

We coherently combine three color components: the  $\lambda_1 = 1030 \text{ nm}$  from a CEP-locked Yb-based femtosecond laser amplifier, its second harmonic at  $\lambda_2 = 515 \text{ nm}$ , and the  $\lambda_3 = 1545 \text{ nm}$  signal wave from a white-light-seeded OPA, pumped by the 1030 nm laser. Superposing these three color components with controlled mutually locked phase delays, we realize a shot-by-shot stable Fourier synthesis of optical cycles, periodically repeated under a  $\approx 180 \text{ fs}$  envelope with  $> 0.5 \text{ mJ}$  total pulse energy. Previous control of HHG has been limited to two colors where these are generally a fundamental + second harmonic [5], which limits the scope for waveform shaping, or a pair of fields of incommensurate frequency with no possibility for systematic phase control [6]. The synthesized optical cycles were used to drive HHG in argon. We have studied how their shape governs the HHG emission by scanning the phase delays  $\tau_2 = \phi_2(\lambda_1 - \lambda_2) / 2\pi c$  and  $\tau_3 = \phi_{\text{CEP}}(\lambda_3 - \lambda_1) / 2\pi c$  of the 515-nm and 1545-nm components, respectively, relative to the 1030-nm base component. Since we aim to observe the steering of the continuum electron wavepacket (EWP), we have normalized the measured HHG spectra by the squared recombination dipole matrix element for argon. Fig. 2 shows these data as function of the laser CEP,  $\phi_{\text{CEP}}$ , for two selected values of  $\phi_2$ , together with EWP intensities simulated with the Lewenstein model using the quantum path analysis [7]. The agreement between the experiment and our single-atom simulations is good over all phase delays, which is proof of

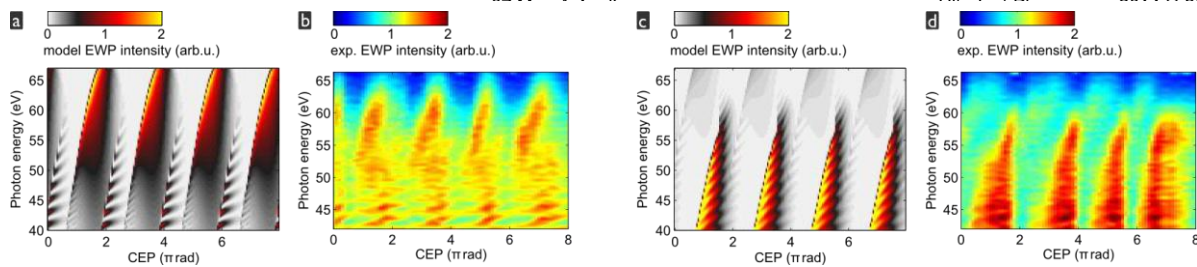


**Fig. 2:** Simulated (a) and measured (b) spectrogram for  $\phi_2=1.2\pi$ ; simulated (c) and measured (d) spectrogram for  $\phi_2=0.6\pi$ . The simulations were performed for a single 10.3-fs long optical cycle using the intensities of the 3 color components as estimated for the measurements. Only the short trajectory family, which is best phase matched in a macroscopic medium, was included. In the experimental spectrograms, the harmonic peak modulation was removed to obtain the spectral envelope. The CEP-values in the experiment have an unknown offset, which could slip between scans for different  $\phi_2$ . Note that  $\phi_2$  may be considered as jitter-free whereas  $\phi_{\text{CEP}}$  jitters by  $\geq 0.95$  rad r.m.s..

direct steering of electron quantum trajectories in HHG via our shaped optical cycles. The clear effect of both varied phase delays shows that the synthesized waveforms survive propagation in the HHG gas medium.

The calculated quantum trajectories show that the ionizing field strength launching the relevant trajectories are optimized, the recollision energies and thus the HHG photon energy cutoff are maximized, and the excursion duration of the relevant trajectories are kept short.

To demonstrate the usefulness of our shaped optical cycles for the cutoff and efficiency enhancement of HHG, we have repeated our experiments at higher driving intensity and thus in the practically most relevant interaction conditions close to saturation. Even under these conditions, we observe clear enhancement of HHG with the synthesized waveforms. Figure 3c shows a measured HHG spectrum generated by a selected optimal waveform. The spectral cutoff clearly lies above the 73 eV absorption edge of the Al-filter used. Figures 3a,b show the HHG spectra generated by sinusoidal drivers. So whilst with the full available OPA output at 1545 nm a fairly high spectral cutoff is achieved, the HHG flux is very low. On the other hand, the laser output at 1030 nm with the same total pulse energy as the three-color waveform leads to saturated HHG with a cutoff below 60 eV, clearly showing the limitations of HHG driven by near-IR drivers. In comparison, the synthesized optimal waveform generates an HHG spectrum that unites high spectral intensities ( $>80$  times increase compared to the mid-IR driver) with a cutoff well beyond the saturation limit of the efficient near-IR driver. The denser harmonic comb spacing leads to even greater enhancement in the integral XUV flux (measured factor  $>140$  in the 55-65-eV range). According to our simulations for the synthesized waveform, the dominant recollision events occur once per 10.3 fs (it would take a 6.2- $\mu\text{m}$  single-color driver to realize the same periodicity), as opposed to once per 2.6 fs in the SWIR case. Consequently, we would expect a several hundred times enhancement in the flux per attosecond burst and thus great implications to future sources of high-energy (isolated) attosecond pulses.

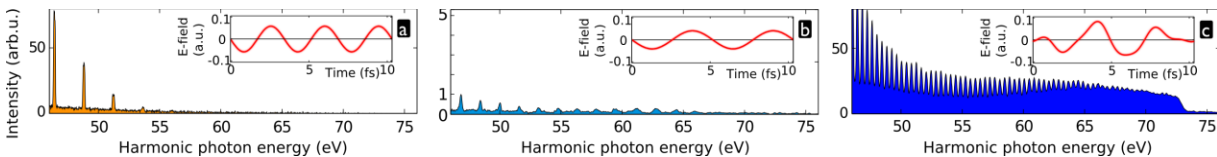


**Fig. 3:** Experimental HHG spectra generated in argon with different driver waves, shown in the insets. The spectral intensities are given on the same scale and are thus directly comparable. (a) 1030-nm driver with the same 0.54 mJ pulse energy as the three-color pulses, leading to the onset of saturation in HHG. (b) 1545-nm driver with the full OPA output pulse energy (0.35 mJ). (c) Chosen 3-colour driver ( $\phi_2=1.8\pi$  and  $\phi_{\text{CEP}}=0.3\pi$ ) giving the highest HHG signal between 60 eV and the Al-filter absorption edge.

Our demonstrated optimization holds significant potential for applications of HHG. Without sacrificing signal intensity for the self-probing of atoms and molecules [8], the desired higher bandwidths of the REWP can be attained even at moderate laser intensities, which is an important requirement for the study of larger molecules or clusters. The corresponding large temporal spacing of the attosecond pulses is of interest in gating techniques for selecting isolated attosecond pulses [9]. The reduced atto-chirp is highly advantageous for the generation of ever shorter and more intense attosecond pulses. It can be compensated with thinner, and thus less absorbing metal filters, thereby further increasing the attainable attosecond pulse energy on target.

Our results demonstrate a new example of many possible applications of cycle-shaped optical waveforms. Every process that is directly laser-field driven will benefit from the possibility of optimization via the shape of the optical cycle. We expect interesting possibilities to emerge in a broad range of laser-matter interaction regimes, involving, e.g., Brunel electrons whose field-driven trajectories can lead to THz-emission [10], plasma heating and HHG on plasma mirrors [11], or particle acceleration [12].

- [1] S.-W. Huang *et al.*, *Nature Phot.* **5**, 475 (2011)
- [2] A. Wirth *et al.*, *Science* **334**, 195 (2011)
- [3] A. Shiner *et al.*, *PRL* **103**, 073902 (2009)
- [4] L. Chipperfield *et al.*, *PRL* **102**, 063003 (2009)
- [5] I. Jong Kim *et al.*, *PRL* **94**, 243901 (2005)

- [7] M. Lewenstein *et al.*, *PRA* **49**, 2117 (1994)
- [8] S. Haessler *et al.*, *J. Phys. B* **44**, 203001 (2011)
- [9] E. Takahashi *et al.*, *Nature Comms.* **4**, 2691 (2013)
- [10] M. Kress *et al.*, *Nature Phys.* **2**, 327 (2006)
- [11] F. Quéré *et al.*, *PRL* **96**, 125004 (2006)